

**REPORT DOCUMENTATION PAGE**

Form Approved  
OMB No. 0704-0188

The public reporting burden for this collection of information is estimated to average 1 hour per response, including the time for reviewing instructions, searching existing data sources, gathering and maintaining the data needed, and completing and reviewing the collection of information. Send comments regarding this burden estimate or any other aspect of this collection of information, including suggestions for reducing the burden, to Department of Defense, Washington Headquarters Services, Directorate for Information Operations and Reports (0704-0188), 1215 Jefferson Davis Highway, Suite 1204, Arlington, VA 22202-4302. Respondents should be aware that notwithstanding any other provision of law, no person shall be subject to any penalty for failing to comply with a collection of information if it does not display a currently valid OMB control number.

**PLEASE DO NOT RETURN YOUR FORM TO THE ABOVE ADDRESS.**

1. REPORT DATE (DD-MM-YYYY) 18092006			2. REPORT TYPE Proceeding		3. DATES COVERED (From - To)	
4. TITLE AND SUBTITLE  Roughness Spectra and Acoustic Response from a Diver-Manipulated Sea Floor				5a. CONTRACT NUMBER		
				5b. GRANT NUMBER		
				5c. PROGRAM ELEMENT NUMBER 0602782N		
6. AUTHOR(S)  Kevin B. Briggs, Michael D. Richardson, Kevin L. Williams, Anthony P. Lyons				5d. PROJECT NUMBER		
				5e. TASK NUMBER		
				5f. WORK UNIT NUMBER		
7. PERFORMING ORGANIZATION NAME(S) AND ADDRESS(ES) Naval Research Laboratory Seafloor Sciences Branch Stennis Space Center, MS 39529				8. PERFORMING ORGANIZATION REPORT NUMBER NRL/PP/7430-06-3		
9. SPONSORING/MONITORING AGENCY NAME(S) AND ADDRESS(ES) Office of Naval Research 800 North Quincy Street Arlington VA 22217-5660				10. SPONSOR/MONITOR'S ACRONYM(S) ONR		
				11. SPONSOR/MONITOR'S REPORT NUMBER(S)		
12. DISTRIBUTION/AVAILABILITY STATEMENT Approved for public release; distribution is unlimited						
13. SUPPLEMENTARY NOTES 1-4244-0115-1/06 2006 IEEE						
14. ABSTRACT  <i>Abstract-A digital stereo photogrammetric system was designed and implemented to measure seafloor roughness in coastal sands. High-resolution images that achieve more than four pixels/mm in either the horizontal or vertical dimension are created by two cameras sealed in watertight housings and actuated simultaneously by a scuba diver. A Digital Elevation Model (DEM) of the photographed sea floor is created from digital autocorrelation of left and right paired images. The DEM is used to estimate a 2D roughness power spectrum, from which are derived parameters of the spectral exponent and spectral</i>						
15. SUBJECT TERMS						
16. SECURITY CLASSIFICATION OF:			17. LIMITATION OF ABSTRACT  SAR	18. NUMBER OF PAGES  5	19a. NAME OF RESPONSIBLE PERSON Kevin Briggs	
a. REPORT Unclassified	b. ABSTRACT Unclassified	c. THIS PAGE Unclassified			19b. TELEPHONE NUMBER (Include area code) 228-688-5518	

# Roughness Spectra and Acoustic Response from a Diver-Manipulated Sea Floor

Kevin B. Briggs and Michael D. Richardson  
Seafloor Sciences Branch  
Naval Research Laboratory  
Stennis Space Center, MS 39529-5004 USA

Kevin L. Williams  
Applied Physics Laboratory  
University of Washington  
Seattle, WA 98105 USA

Anthony P. Lyons  
Applied Research Laboratory  
The Pennsylvania State University  
State College, PA 16804-0030

**Abstract**—A digital stereo photogrammetric system was designed and implemented to measure seafloor roughness in coastal sands. High-resolution images that achieve more than four pixels/mm in either the horizontal or vertical dimension are created by two cameras sealed in watertight housings and actuated simultaneously by a scuba diver. A Digital Elevation Model (DEM) of the photographed sea floor is created from digital autocorrelation of left and right paired images. The DEM is used to estimate a 2D roughness power spectrum, from which are derived parameters of the spectral exponent and spectral strength that are used as inputs in high-frequency acoustic scattering models.

## I. INTRODUCTION

An important component of the Sediment Acoustic EXperiment 2004 (SAX04) conducted in the northeastern Gulf of Mexico during September–November of 2004 was to investigate the acoustic scattering from the rippled sea floor. In situ manipulative experiments were conducted to determine the effects of dynamic seafloor roughness on high-frequency acoustic scattering, with particular emphasis on the effects of degradation of sand ripples on temporal decorrelation of scattering strength measurements. This experiment was conducted in moderately well sorted, medium quartz sand (mean diameter: 0.360 mm) with 40- to 95-cm wavelength sand ripples. The site was located about 1.4 km offshore of Fort Walton Beach, Florida in 16.5 m of water [1].

The experimental approach for ascertaining the effects of changing seafloor roughness on acoustic scattering was to have divers deliberately rake the sand surface in situ with saw-tooth tools, creating quasi-sinusoidal microroughness with spacing between adjacent ridges of 1.92 cm and height of about 1 cm. The spacing was chosen to approximate half of a

wavelength corresponding to an acoustic frequency of 45 kHz—*i.e.*, the Bragg wavelength for 45 kHz. Ripple-like patterns were created for treatments parallel, perpendicular, and 30 degrees to the transmitted direction of acoustic energy from a variable frequency (20 to 150 kHz) transducer mounted on a 4.8-m-high, moveable, underwater tower. Divers made the ripple patterns in a 2 m-by-2 m quadrat 10 m from the tower, resulting in a grazing angle of about 28 degrees to the desired target. Upon creating the microroughness, and subsequently thereafter at various time intervals, divers were to document the seafloor morphology with underwater photogrammetry.

Prior to and during SAX04 Hurricanes Frances, Ivan, and Jeanne, as well as Tropical Storm Matthew, interrupted the collection of data. Furthermore, underwater visibility during the experiments was hampered by material suspended in the water from these storms that rendered photogrammetry ineffectual. In addition to the lack of water clarity, another obstacle encountered was a result of the most intense of the storms (Ivan) coming ashore within 100 km of the experiment site—the draping of lagoonal mud onto the surface of the sand [2]. Subsequent reworking of the mud deposit by wave action created a patchy distribution of mud and sand that presented a non-uniform surface from which to collect environmental and acoustic data. Although the divers were able to manipulate the sea floor and the acoustic data were collected, only a few photographs of the sea floor were taken and none of them depicted the raked microroughness or the degraded raked microroughness. As a consequence of the poor visibility and less-than-pristine sand sea floor encountered during SAX04, digital stereo photography was planned to be conducted by divers on re-creations of the manipulations when water clarity improved sufficiently for high-resolution photogrammetry at the same site.

---

This work was supported by the Office of Naval Research, Ocean Acoustics Program and by the Naval Research Laboratory, program element N602782N.

From the digital stereo photographs the 3D surface of the sea floor can be realized; from the 3D realization a 2D roughness power spectrum can be estimated; from the roughness power spectrum the spectral exponent and spectral strength parameters corresponding to the slope and intercept of regression lines calculated at the appropriate azimuths of the roughness orientations can be derived [3]; and from the two parameters describing the roughness spectrum at the appropriate orientations inputs to acoustic scattering models can be determined [4]. Ultimately, the predictions of the scattering models can be compared with the acoustic scattering data collected during SAX04.

## II. DESCRIPTION OF CAMERA SYSTEM

The digital stereo camera system is constructed of two Kodak DCS Pro SLR/n digital cameras with 28-mm Nikkor lenses mounted in watertight aluminum canisters with 15.2-cm-diameter dome ports (Fig. 1). The dimensions of the canisters (wall thickness = 2.54 mm) provide a maximum operable water depth in sea water (287 m) well beyond the depth limit of the acrylic dome ports (61 m) as well as scuba diving limits (30-40 m). The two 18.5-cm-long, 23-cm-diameter cylindrical canisters are separated by a 47.5-cm distance measured from left and right camera image planes. These canisters containing the cameras are tilted inward toward each other at 10 degrees from vertical to ensure a 95×67-cm image overlap area at a distance of 96 cm from the sea floor.

Two Ikelite 110-watt-second strobes mounted on either side of the 2.7-cm-diameter, tubular aluminum frame provide sufficient lighting for the image pairs. The strobes are configured to be 72 cm from the subject and the 79 cm from the camera and at a low angle, by having the right camera image illuminated from the left strobe and vice versa. This configuration avoids “hot spots” from having the strobe too close to the subject, yet affords reduced scattering from suspended matter in the water by allowing the light to approach the subject at a shallow angle 44 cm from the sea floor. Each camera is manually set before the dive at an ISO setting of 160, a shutter speed of 1/60 s, and an f-stop of 16. These settings balance a minimum of image noise with an acceptable depth of field in the image. The strobe flash intensity is adjustable, with adequate lighting achieved at half intensity in water depths less than 10 m (in daylight) and full intensity below 10 m. The focal length setting on the 28-mm lenses is manually fixed at the distance determined from the “autofocus” feature when operating the system underwater in a test tank. In this way, the precise focal length of the lenses for photogrammetry calibration is determined to a hundredth of a millimeter. The lens ports are not flat, thus obviating “port-vignetting” and “pincushion distortion” that reduce the angle of coverage of the recorded image. The dome-shaped port is a concentric lens that acts as an additional element to the AF Nikkor 28-mm F/2.8D camera lens. Use of dome ports significantly reduces problems of refraction, radial distortion, and axial/chromatic aberrations that affect image quality.



Figure 1. The NRL digital stereo camera system mounted on a tubular aluminum frame and including two Ikelite strobes mounted outboard of the 95×67-cm overlap field of view.

The cameras and strobes use separate, rechargeable batteries and each camera writes 13.5-megabyte (4500 by 3000 pixels) images to removable memory cards capable of storing up to 1.5-gigabytes in each camera. In practice, the compact flash and multi media cards in each camera together will accept nearly 100 images. Thus, the digital photogrammetry can be conducted independently by divers and free from constraints presented by cables or tether to ships. The weight in water of the entire system is only 4.1 kg, due to the buoyancy provided by the canisters and the tubular, 28-mm-diameter, aluminum frame. Both cameras and both strobes are actuated nearly simultaneously by a diver-operated, spring-loaded button on the handle located centrally above the canisters. The time lag between image collection of the two cameras is a fraction of a second and should not allow changes to the sea floor to occur during the lag that would cause errors in the generation of a digital elevation model. The buoyancy, weight distribution, and drag of the camera system are designed to minimize diver effort during swimming to conduct the close-range underwater photography.

The imaging sensor used in the digital cameras is a 12-bit Complementary Metal Oxide Semiconductor (CMOS) that covers a 24-by-36-mm image area, equivalent in size to 35-mm film. This imager enables wide-angle, digital, underwater photography without the focal length magnification that occurs with a Charge-Coupled Device (CCD) and provides sufficient resolution for characterizing microroughness relevant to high-frequency acoustic scattering [5]. At the full resolution at

which the camera sensors are capable, images are composed of just over four pixels per mm. CMOS sensors also require less power than CCD sensors, thus allowing for practical application of digital cameras for battery-powered operations where the power demand extends from when the cameras are sealed in the canisters until the last photograph is taken.

Other important features of the digital camera system include a digital directional compass with an LCD and shades protecting the dome ports. The compass can be mounted on a horizontal section of the frame in the field of view aligned such that the diver is facing the direction indicated on the LCD. It provides the orientation (in 5° increments) of the photographs, which is valuable for relating anisotropic seafloor roughness orientation to acoustic projector azimuth. The dome port shade provides not only a reduction of refracted light into the camera sensor from the water but protection of the surface of the plastic dome from scratches.

### III. CALIBRATION AND DEM PRODUCTION

Images written to the memory cards are saved as "raw" Kodak proprietary files. These proprietary files are converted to Tagged Image File Format (TIFF) via Kodak software before processing of the images for photogrammetry can proceed. The TIFF is preferable to JPEG format, which, due to compression of the image, causes unequal file sizes for the left and right stereo images. Before the 2D height field, or Digital Elevation Model (DEM), is produced from the stereo images, the images must be rectified and the resultant images must undergo a stereo correlation.

Image rectification is essential for stereo image systems that have a convergent geometry as the NRL system has. In image rectification the image is transformed such that the effects of camera orientation with respect to the sea floor are removed. The transformation process depends on known corresponding

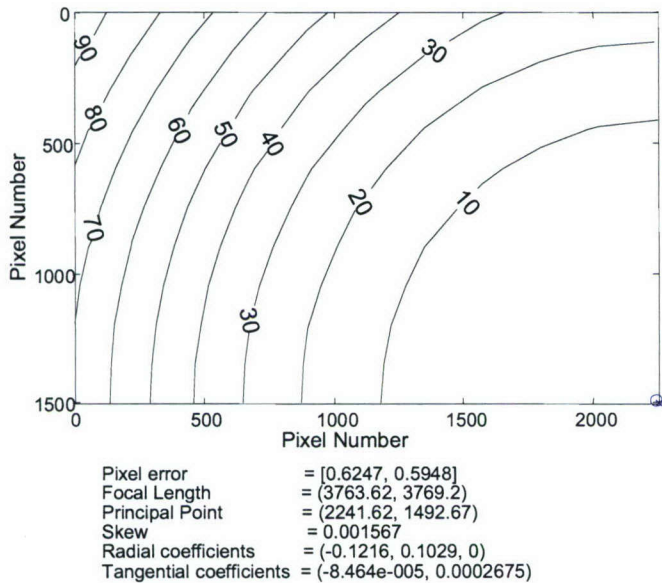


Figure 2. Distortion model (upper left quadrant) for the left camera. Image center and principal point (right, bottom) are marked "x" and "o", respectively.

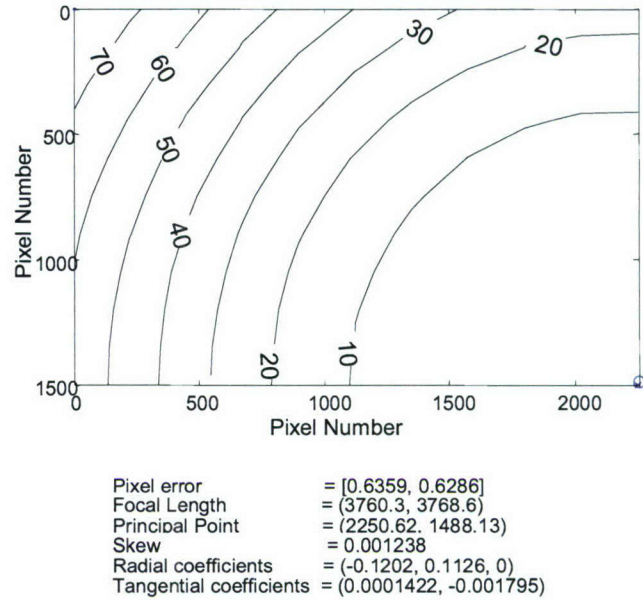


Figure 3. Distortion model (upper left quadrant) for the right camera. Image center and principal point (right, bottom) are marked "x" and "o", respectively.

points of the stereo paired images. Before the corresponding points are established, the camera images must be calibrated for distortion in the camera lenses.

In order to calibrate the two cameras of the digital stereo camera system, a checkerboard pattern composed of 5-cm black and white squares was affixed to a glass plate and photographed underwater. The checkerboard pattern, visible from both cameras, was used to construct left and right distortion models from which the intrinsic and extrinsic parameters of the cameras are calculated using Bouquet's camera calibration toolbox [6]. The contours in Figs. 2 and 3 are lines of equal displacement between original distorted image coordinates and corrected image coordinates (only one quadrant from each camera is shown). The interior camera parameters obtained by the calibration algorithm are listed below each quadrant. The exterior, interior, and distortion parameters from each camera are essential for calculation of errors.

The errors are differences (in pixels) between extracted grid corner coordinates and the respective coordinates calculated by re-projecting the known grid-corner positions using the set of exterior, interior and distortion parameters. An example of the re-projection of grid points for one of the left calibration images is shown in Fig. 4. The extracted grid corners are marked with red crosses and the grid corner positions calculated by re-projection are marked with blue circles. The deviation of the image of the grid from the green lines, which are orthogonal, straight lines, indicates some slight radial distortion in the image. A close-up view of the effects of radial distortion on the camera image is shown in Fig. 5, where the deviation of the grid appearance from the orthogonal green lines, as well as the differences between the location of the grid corners and the location of the re-projected grid corners are apparent.

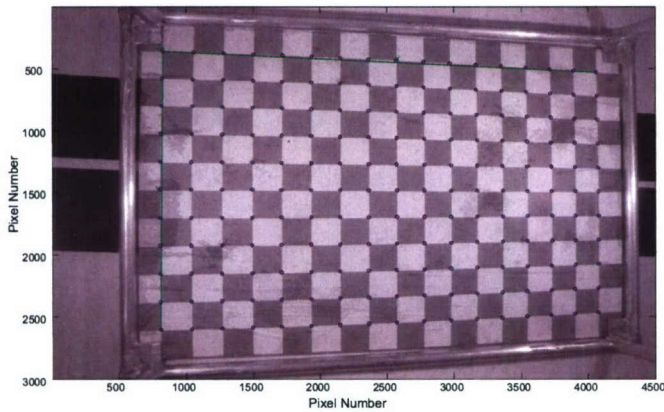


Figure 4. Re-projection of grid points for one of the left camera images of the 5×5-cm calibration grid.

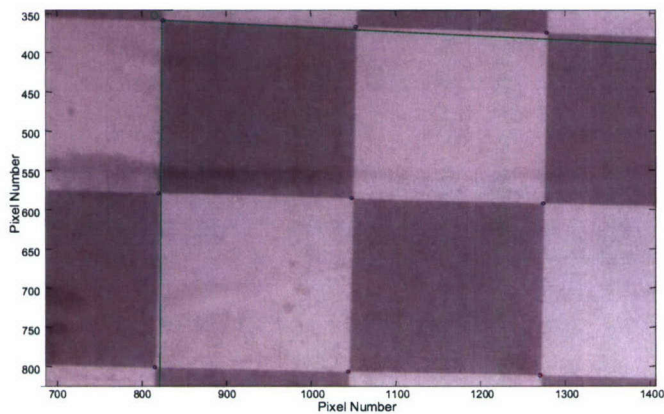


Figure 5. Close-up view of Fig. 4 to show the error due to distortion.

Calibration photos were taken in five positions (flat; and tilted left, right, top and bottom) with respect to the fixed geometry of the camera system. The distribution of the error between the real corner and the re-projected corner at each grid vertex for all positions and duplicates indicates a relatively tight cluster with some outlying values (Figs. 6, 7).

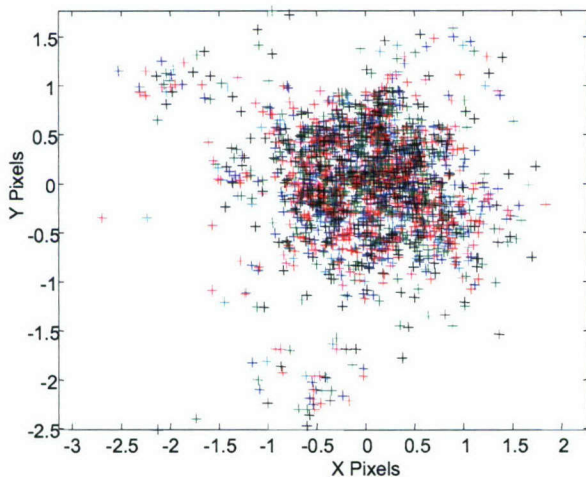


Figure 6. Re-projection errors for the left camera image. Different color symbols indicate different positions of the calibration grid.

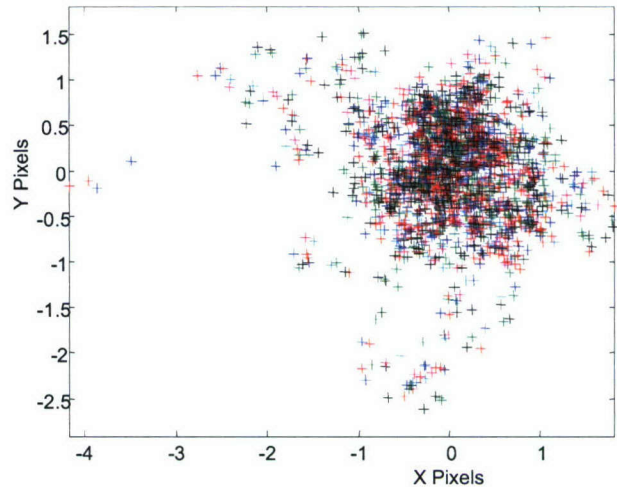


Figure 7. Re-projection errors for the right camera image. Different color symbols indicate different positions of the calibration grid.

Once the calibration of the images has been completed the images undergo registration, in which the orientation effects are removed. Comparison of the left and right registered images with automatic stereo correlation, using a technique called area-based matching, results in the derivation of the relative height differences of the photographed sea floor [3].

#### IV. SEAFLOOR MANIPULATION AND DOCUMENTATION

Photographs of raked sand were collected from Vortex Springs, FL in December 2005 and from south of the SAX04 site in May 2006 (Figs 8, 9). A recent algae bloom degraded under-water visibility near the sea floor at the SAX04 site, rendering the photographs useless for photogrammetry. Digital Elevation Models composed of 3D arrays of position ( $x, y$ ) and height ( $z$ ) values were constructed from autocorrelation of digital image pairs from the Vortex Springs site. 2D roughness power spectra are estimated from the array values, taking care to taper the data array to reduce spectral leakage [3]. These 2D roughness spectra are expected to quantify the regular ripple-like patterns created by the divers in terms of roughness power ( $\text{dB}\cdot\text{cm}^4$ ) as



Figure 8. Left camera image of raked sand at Vortex Springs, FL on December 1, 2005. Spacing between grooves is 1.92 cm.



Figure 9. Right camera image of raked sand near the SAX04 site off Ft. Walton Beach, FL on May 22, 2006. Note scatter from suspended matter in water that degraded the image.

a function of 2D spatial frequency. Slices through the 2D power spectra yield azimuth-dependent periodograms of 2D roughness power as a function of spatial frequency that resemble 1D power spectra. The slope and intercept of power-law regressions from these periodograms can be used as parameters of spectral exponent and spectral strength, respectively, for estimating scattering strength as a function of azimuth angle from the first-order, small-roughness perturbation model.

The manipulative experiments that were conducted in SAX04 on 18-19 October allowed the following quantitative analysis of the backscattering data (20-90 kHz) and comparison to model simulations. A plot of backscattering strength as a function of grazing angle shows a strong peak in scattering strength at 45 kHz for the grazing angles between 25° and 30° (Fig. 10). Grazing angles at which these peak scattering strengths were measured correspond geometrically to the angle from the acoustic transducer to the area raked by divers. The tine spacing of 1.92 cm should create the same spacing in the

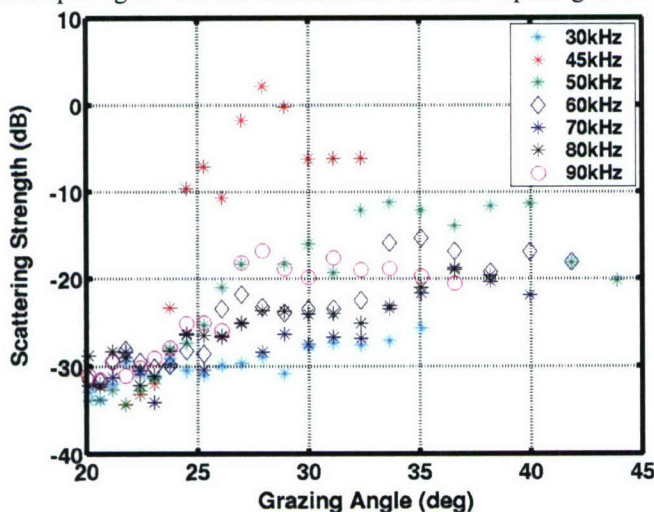


Figure 10. Backscattering strength as a function of grazing angle measured over the frequency range 30-90 kHz from the raked sea floor at SAX04.

diver-generated ripples, and this regular microtopography should be reflected in the 2D roughness spectrum as a definitive peak in the spatial frequency domain at 0.52 cycles/cm. The wavelength of the “artificial” ripples is approximately the “Bragg wavelength” given by  $\lambda/2 \cdot \cos\theta$  for 45 kHz, where  $\theta$  is the incident angle.

Model predictions of scattering strengths were made for the various acoustic frequencies as a function of grazing angle using the parameters from 2D roughness spectra generated from a previous (SAX99) set of roughness data. The largest peak in predicted scattering strength occurred at the frequency of 45 kHz at the grazing angle of 28 degrees corresponding to the location of the raked sea floor experiment [7]. This predicted peak is about 20 dB above predictions for the frequencies above and below the Bragg resonant frequency.

Although the predicted scattering strength compares closely with the measured scattering strength, there are some uncertainties due to measurement errors. More rigorous model-data comparisons would require the processing of the most recent digital stereo photographs taken at Vortex Springs. Estimation of the 2D roughness power spectrum from the DEMs produced from stereo correlation of images of the raked sea floor would eliminate the uncertainty in the value of the width of the spectra peak representing the “artificial” ripple and would allow an examination of frequency dependence in the model.

#### ACKNOWLEDGMENT

C. Kennedy, D. Young, and G. Bower were responsible for the construction of the camera system and calibration plate. We thank R. Ray, C. Vaughan, D. Lott, T. Hefner, E. Boget, P. Aguilar, E. Kloess, and J. Piper for diving support during SAX04. We also thank the captains and crew of the R/V Pelican, R/V Seward Johnson, and M/V Aquanaut for ship support. Contribution no. NRL/PP/7430-06-3.

#### REFERENCES

- [1] M. Richardson, K. Briggs, A. Reed, W. Vaughan, M. Zimmer, L. Bibee, and R. Ray, “Characterization of the environment during SAX04: Preliminary results,” in *Underwater Acoustic Measurements: Technologies and Results*, J.S. Papadakis and L. Bjørnø, Eds. Heraklion, Crete, Greece: F.O.R.T.H., 2005, pp. 285-292.
- [2] K. Briggs, and A. Reed, “Using CT to image storm-generated stratigraphy in sandy sediment off Fort Walton Beach, Florida, USA,” in *Underwater Acoustic Measurements: Technologies and Results*, J.S. Papadakis and L. Bjørnø, Eds. Heraklion, Crete, Greece: F.O.R.T.H., 2005, pp. 95-102.
- [3] A. Lyons, W. Fox, T. Hasiotis, and E. Pouliquen, “Characterization of the two-dimensional roughness of shallow-water sandy seafloors,” *IEEE J. Oceanic Engin.*, vol. 27(3), pp.515-524, July, 2002.
- [4] K. Briggs, “Microtopographical roughness of shallow water continental shelves,” *IEEE J. Oceanic Engin.*, vol. 14 (4), pp.360-367, October, 1989.
- [5] K. Briggs, A. Lyons, E. Pouliquen, L. Mayer, and M. Richardson, “Seafloor roughness, sediment grain size, and temporal stability,” in *Underwater Acoustic Measurements: Technologies and Results*, J.S. Papadakis and L. Bjørnø, Eds. Heraklion, Crete, Greece: F.O.R.T.H., 2005, pp. 337-344.
- [6] J.-Y. Bouguet, Camera calibration toolbox for Matlab. Available from: [http://www.vision.caltech.edu/bouguetj/calib\\_doc/](http://www.vision.caltech.edu/bouguetj/calib_doc/)
- [7] M. Richardson, K. Briggs, K. Williams, D. Tang, D. Jackson and E. Thorsos, “The effects of seafloor roughness on acoustic scattering: manipulative experiments,” in *Boundary Influences in High Frequency, Shallow Water Acoustics*, N.G. Pace and P. Blondel, Eds. Bath, UK: Univ. of Bath, 2005, pp. 109-116.

Welcome

Sessions

Final Program

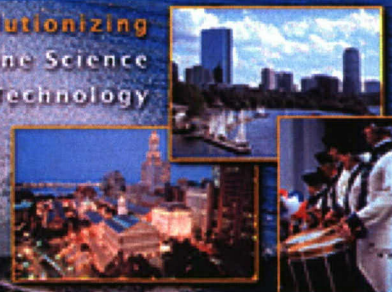
Authors

Search

MTS • IEEE  
2006  
**OCEANS**  
BOSTON

September 18-21, 2006 • Hynes Convention Center, Boston, Massachusetts

Revolutionizing  
Marine Science  
& Technology



© 2006 IEEE. Personal use of this material is permitted. However, permission to reprint/republish this material for advertising or promotional purposes or for creating new collective works for resale or redistribution to servers or lists, or to reuse any copyrighted component of this work in other works must be obtained from the IEEE.

IEEE Catalog Number: 06CH37757C

ISBN: 1-4244-0115-1

Library of Congress: 2005938570

Additional copies of this publication are available from

Marine Technology Society, 5565 Sterrett Place, Suite 108, Columbia, MD 21044 USA

Tel: +1 410-884-5330, Fax +1 410-884-9060, email: [mtsmbrship@erols.com](mailto:mtsmbrship@erols.com)

IEEE Operations Center, P.O. Box 1331, 445 Hoes Lane, Piscataway, NJ 08855-1331 USA

Tel: +1 800 678 IEEE, Fax: +1 732 981 9667, email: [customer-services@ieee.org](mailto:customer-services@ieee.org)

Adobe and Acrobat are trademarks of Adobe Systems Incorporated or its subsidiaries and may be registered in certain jurisdictions. Macintosh is a registered trademark of Apple Computer, Inc. UNIX is a registered trademark in the United States and other countries, licensed exclusively through X/Open Company, Ltd. Windows is a trademark of Microsoft Corporation. I386, I486 and Pentium are trademarks of Intel Corporation.

Produced by Veraprise Incorporated

For technical inquiries, please contact: Veraprise Incorporated, P. O. Box 949 Front Royal, VA 22630

Tel: +1 540-631-0919, Fax: +1 540-631-3464, <http://www.veraprise.com/>, [support@veraprise.com](mailto:support@veraprise.com)

**Using the SEARCH tool:** The **Search** button on this page and the **Search** link in the bookmark panel on the left will start an Adobe PDF Search panel if you are running Version 7 of Acrobat Reader. If you are running an earlier version of Acrobat Reader you will need to click the **Search** icon in the toolbar at the top of this window or select **Search** from the **Edit** menu to start the PDF Search panel. Alternatively, you may wish to install Version 7 of the Acrobat reader, which is included on this CD.